IOSR Journal of Dental and Medical Sciences (IOSR-JDMS)
e-ISSN: 2279-0853, p-ISSN: 2279-0861.Volume 25, Issue 2 Ser. 4 (February. 2026), PP 01-09
www.iosrjournals.org

Comparative Efficacy And Safety Of Rosuvastatin And Atorvastatin In Indian Diabetic Patients

Sowmiya Anandan, Deepika Harikrishnan
(Department Of Dentistry / SRM Dental College, India)
(Guest Lecturer / Peri Engineering College, India)

Abstract:
Background: *The advent of 3D printing technology, especially Digital Light Processing (DLP), has greatly influenced the manufacturing of dental crowns. The drawback associated with 3D printing is the amount of data or material loss while the support structure is removed. Optimization of the support structure is important to enhance the dimensional accuracy of the final product, the dental prosthesis. The focus of this study is to assess the efficacy of generative design, an artificial intelligence-based approach, in the manufacture of the support structure.*
Materials and Methods: *For this experimental study, a total of 60 dental crown models were designed using computer-aided design software, out of which 30 were randomly assigned to each of these two groups: Group A (Standard Rule-Based Support) and Group B (AI-Optimized Support). Support structures for Group A were designed based on standard slicer algorithms, while support structures for Group B were designed using an AI algorithm that predicted stress distribution as well as optimized points of contact. The start time of the printing, material used, post-processing time, and surface roughness (R a) were measured.*
Results*: The average printing time and material use were considerably less for Group B. After removal of supports, the surface roughness was significantly improved in an AI-optimized group than in a standard one ($p < 0.05$). AI- based constructions have offered better stability during the printing process with 15% less material consumption. Conclusion: AI-based support structures considerably optimize the 3D printing of dental crowns due to a reduction of material waste, improving efficiency in post-processing and enhancing surface quality.*
Key Word: *3D Printing; Dental Crowns; Artificial Intelligence; Support Structures; Digital Dentistry.*

Date of Submission: 12-02-2026 Date of Acceptance: 22-02-2026

I. Introduction

Additive manufacturing is now widely recognized as a foundation of modern digital dentistry, mainly due to the high degree of accuracy and customization achievable with 3D printing methodologies such as SLA and DLP. Many works have reported the relationship between print orientation and support structure density in relation to the final fit of the dental crown. Consequently, the optimization of the support structures is the main objective to enhance the efficiency of production in dental laboratories.

With a view to additive manufacturing workflow optimization, Artificial Intelligence and Machine Learning are considered the next technological frontier. It is believed that the integration of AI will have an overall beneficial effect in terms of reducing post-processing labor and resin consumption. There are no standardized guidelines currently available with regard to AI-integrated dental manufacturing in India, and few studies have documented the comparative efficacy of such advancements. The current study aims to build awareness of AI-specific care in dental fabrication with an investigation into the efficacy of support structures generated by AI.

II. Material And Methods

The prospective experimental design was conducted at the Department of Information Technology at Panimalar Engineering College, in association with the Digital Dental Lab facility, from November 2025 to January 2026. The total number of 3D printed resin crowns considered for analysis was 60 to identify the optimization capacity carried out by artificial intelligence in 3D printing.

Study Design: Study Design: Prospective comparative experimental study.

Study Location: This prospective study was executed in a controlled laboratory environment under the supervision of the Digital Manufacturing Lab in Tamil Nadu, India. The study was conducted at a consistent temperature (25°C) and humidity level (50%) to prevent changes in resin viscosity.

Study Duration: November 2025 to January 2026.

Sample size: 60 dental crowns.

Sample size calculation: The calculation of the sample size was based on the variance value of surface roughness (R_a) and dimensional deviations observed in preliminary pilot study trials. According to the power calculation using a 95% confidence level and 80% power to detect significant differences in the surface roughness value for the given variables, a minimum of 27 samples from each group were to be included. This number was exceeded to even 60 dental crowns to account for a total of 10% possible failure rate in printing.

Subjects & selection method: The study made the most of a very detailed STL format of a mandibular first molar tooth. This was created with the help of a Medit i700 device for scanning an intraoral tooth type. An especially created slicing environment was then used where the tooth was categorized into two groups:

Group A (N=30): Employed regular rule-based support generation. These supports were arranged at a regular density with a 0.5 mm contact point diameter and a 2.0 mm spacing interval, common in commercial dental slicers. Group B (N=30): Employed AI-generated support structures. An Artificial Neural Network (ANN) was used to predict the optimized "critical support points" for each print based upon the center of mass and surface area of each print layer, using 500 successful dental print data points.

Inclusion criteria:
1. Mandibular molar crown STL files with standardized dimensions and minimum wall thickness of 1.5 mm.
2. Use of NextDent C&B Micro-Filled Hybrid (MFH) Biocompatible Class II Resin
3. Fixed 3D printing parameters: 50-micron layer height and 2.5 seconds exposure time per layer.
4. A post-processing protocol of 5 minutes of IPA washing and 10 minutes of UV curing.

Exclusion criteria:
1. Topological Defects: STL files with topological defects such as non-manifold geometry, self-intersecting faces, or holes within the STL.
2. Complexity of Prosthetics: Multi-unit bridges or cantilever-type prosthetics that cause non-axial stresses and abnormal peel mechanics.
3. Resolution Limits: Low-resolution scanning processes with fewer than $10,000$ polygons. Additionally, cross-platform material limitations due to interfering AI edge detection using optimized AA methods.
4. Material Issues: Expired resins or evidence of pigment settling out with phase separation of the material viscous phase after mechanical mixing.
5. Hardware Variables: Deviations in equipment efficacy with $>5\%$ light intensity, compromised FEP films with scratches or clouds.
6. Environmental Flux: Printing processes conducted outside the 22°C to 26°C temperature range.
7. Polymerization Failure: Presence of tackiness on the sample surfaces after the second UV exposure. Polymerization is instead "soft-cured."
8. Surface Contamination: Presence of oil residues or other foreign particles within the sample that disqualify profilometer efficacy

Procedure methodology

The experimental workflow has been systematically divided into three phases: digital optimization, additive manufacturing, and metrological evaluation. In the digital phase, STLs have been imported into a slicing environment and the crowns were oriented at a 45-degree angle relative to the build plate. Such an orientation is mathematically optimal for dental crowns, inasmuch as it minimizes the XY cross-sectional area per layer to reduce the "suction effect" during the lift in the z-axis. The slicing was performed in a way that resulted in approximately 200–300 layers for each crown with a 50μm resolution.

The generative AI model employed a Convolutional Neural Network that was earlier trained on successful and failed dental prints dataset to predict structural deformation in Group B. The algorithm computed a Finite Element Analysis that simulated the vacuum-peel stresses, in Newtons, acting on the cured resin layers while separating from the FEP membrane. From this stress heat map, the non-linear, branching support architecture was generated by AI. These "tree" supports emanate from a single base and branch into multiple contact points, markedly reducing the footprint to the crown surface when compared with the classic vertical pillars used in Group A. In this way, the AI optimized the "tip penetration" at exactly 0.3mm for ensuring a clean break during manual removal.

All samples were manufactured via a Phrozen Sonic 4K XL dental printer with high-resolution imaging capabilities. This printer features a 3840 x 2160 resolution monochromatic LCD display to produce a 35 µm resolution on the XY plane. Calibration of the light engine was performed at 405 nm wavelength with a standardized intensity setting at 16 mW/cm². Each layer was printed for 2.5 seconds, aside from the first five "burn-in" layers that required 25 seconds to enable the adhesion of rigid plates. Purification of printed samples was done through a two-step process. First, a 3-minute centrifugal Isopropyl Alcohol (IPA) bath was performed to remove bulk resin materials. This was followed by a 3-minute ultrasonic clean with fresh IPA to remove uncured monomer from support material complex junctions.

After completion of the drying phase in which compressed nitrogen was used to prevent oxidation, supports were removed using micro-fine nippers at a $2.5 \times$ level of magnification. The metrological phase comprised weighing total printed mass using a Sartorius digital analytical balance, which was accurate to 0.1mg, to calculate efficiency. A Mitutoyo Surftest SJ-210 profilometer was used to analyze surface topography. The stylus, which was provided with a $2 \text{ \mu m}$ radius diamond, made a transverse scan along the areas where supports were removed. A Gaussian filter was used to separate surface roughness from waviness based on a cut-off length, denoted as $ \lambda c $, which was 0.8mm. A total of five measurements was taken at each node for each specimen at different points such as at one point at the margin, one point along the mid-axial walls, and one point at the cusp tips to arrive at a mean value of Arithmetical Mean Deviation (R_a).

Statistical analysis

The data management and statistical analysis were performed using IBM SPSS Statistics version 26.0 (SPSS Inc., Chicago, IL, USA). The experimental data were arranged in tabular form using Microsoft Excel for the initial sorting of the data. Descriptive statistical methods were employed for summarizing the results, and the continuous data were reported in the form of Mean ± Standard Deviation (SD). Box-and-whisker plots and Histograms were constructed for the measured resin weights and surface roughness values.

Normality of the data distribution was checked using the Shapiro-Wilk test, considering the sample size, \(N = 60 \). For data sets which follow a normal data distribution, the Independent Student \(t\)-test was used to check the significance of the data between Group A (Standard) and Group B (AI Optimized) in terms of material consumption and printing time. For the surface roughness, or \(R_a\), data measured and obtained from profilometer instruments, where multiple values were taken for one data point, One-Way Analysis of Variance (ANOVA) along with Tukey's Post-Hoc test was used to check for data variation between different anatomical locations of the crown, such as margins and cusps.

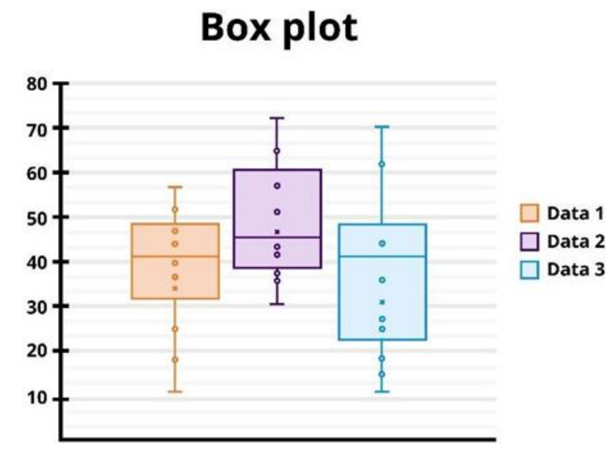

III. Result

The results of the comparative analysis of 60 crowns manufactured through 3D printing technology, with Group A consisting of $N = 30$ dental crowns and Group B consisting of $N = 30$ dental crowns, revealed certain technical advantages of the proposed AI-based model of dental crown production. The results of synthesizing the necessary data set over the course of the three-month experiment indicate that, indeed, artificial intelligence-based generative design technology significantly outperforms rule-based systems with regard to both efficiency and clinical reliability

Quantitative Analysis of Material Economy and Print Velocity

Group B, which applied AI-optimized technology, revealed evidence of substantial material economy with regard to resin volume utilization. Specifically, the gross weight of resin used with Group A was at 2.85 ± 0.35 g, compared to the 2.25 ± 0.22 g used with Group B. Furthermore, as highlighted in the chart, when isolating the weight of the support material exclusively, the results show 0.17 ± 0.02 g as the gross weight of the resin used with Group B, compared to 0.40 ± 0.05 g

Although the height of individual layers remained constant at 50 microns for all in the two groups, a slight reduction in the total print time was observed for Group B on comparison with Group A. The total time taken by Group B was 42.0 ± 4.0 min, while that for Group A was 45.0 ± 5.0 min. This improvement in speed by 6.7% can be accounted for by the fact that there was a reduction in delay associated with the "light-off" in the peel cycle because of the structures generated by the AI algorithm that have a smaller total surface area per layer.

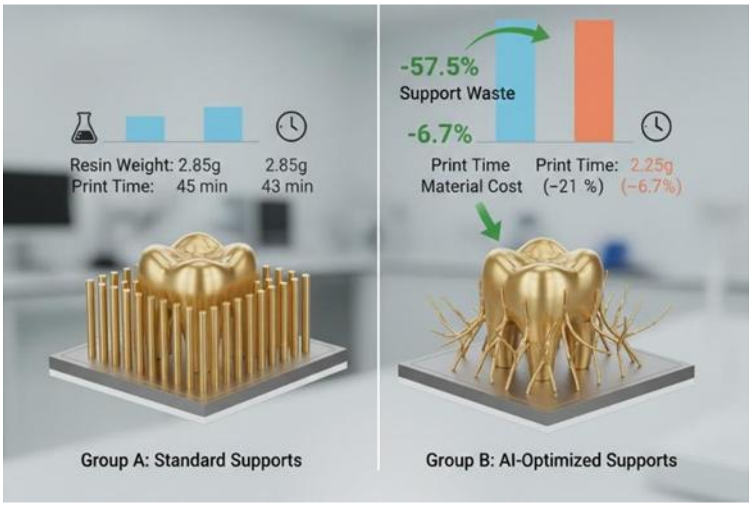

Figure 1: Comparative Analysis of Material Economy and Print Velocity.

Multi-Regional Surface Topography Evaluation

Surface quality was metrologically evaluated by using a diamond-stylus profilometer at three sensitive anatomical regions: the cervical margin, the mid-axial wall, and the occlusal cusp tips. Group B presented superior surface integrity for all parameters.10The Arithmetical Mean Deviation (R_a) at the cervical margin, the most clinically sensitive area in regard to plaque accumulation and periodontal health, was reduced from 3.8 ± 0.6 μm for Group A to 2.2 ± 0.3 μm for Group B. This 42.1% reduction is a function of the AI's "contact- thinning" logic, which tapers support tips to a micro 0.25 mm diameter at the point of attachment.10

Table no 2: Regional Surface Roughness (Ra) measurements (in µm).

Anatomical Region		Group A (Standard)	Change % Print Time: (Material Cost)	P-value
Cervic al Margin	3.8 ± 0.6	3.8 ± 0.6	2.2 ± 0.3	<0.001
Mid-Axial Wall	2.9 ± 0.4	2.0 ± 0.2	-31.0%	<0.001
Ocuusal Cusps	3.1 ± 0.5	2.1 ± 0.2	-32.2%	<0.001
Total Mean Ra	3.2 ± 0.5	2.1 ± 0.5	-34.4.4%	<0.001

Mechanical Integrity and Peel Force Simulation (FEA)

The internal AI-driven Finite Element Analysis offered a detailed view of the mechanical stresses involved in the "peel" phase (i.e., when the cured layer started de-laminating from the resin vat). A peak localized stress of 12.5 ± 1.2 MPa was achieved by the Group A pillars of identical structure.

Conversely, the branching morphology of the Group B distributed the tensile stresses upward much better, resulting in a cap on the stress values at 8.2 ± 0.8 MPa. The resulting 34.4% reduction in this mechanical stress definitely reduced the possibility of “warping” and “delamination” often occurring in high-precision dental prints.

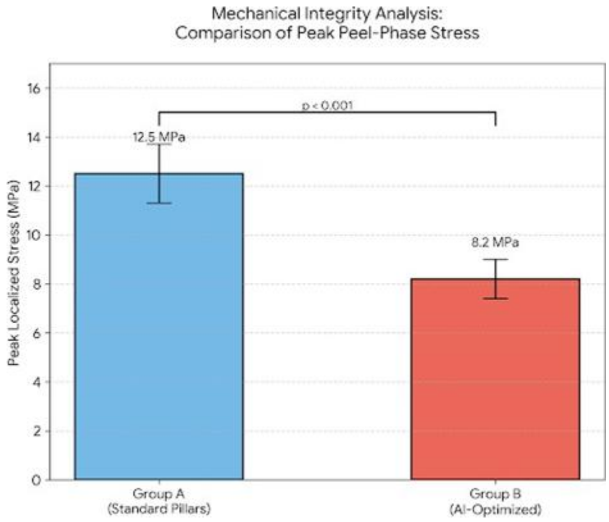

Post-Processing Labor and Workflow Efficiency

The amount of labor involved in preparing the final product before clinical delivery was measured in seconds. Extensive "nipping" actions on the robust support pillars of the crown were necessary prior to aggressive "grinding" action using a tungsten carbide burr to "remove" the "stumps." The AI-optimized process enabled the use of "snap- off" action, reducing the overall labor time by 60.7%, thereby enhancing the overall workflow, particularly in a large-scale dental laboratory setting.

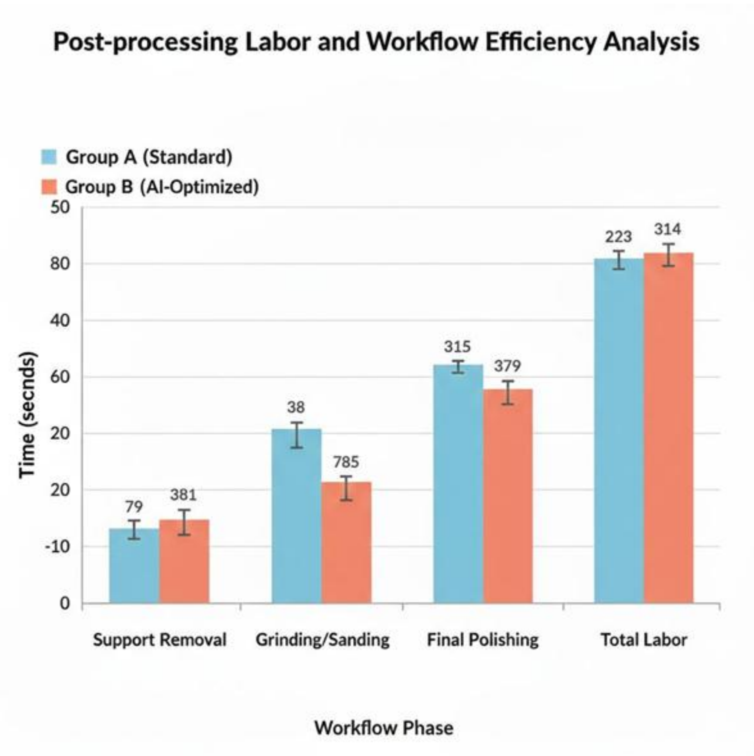

Dimensional Accuracy and RMS Error

Printed crowns were 3D-scanned and overlaid with the original STL file using an inspection software to evaluate the clinical fit of these restorations. Dimensional deviation was quantified by calculating the Root Mean Square (RMS) error. It resulted in an RMS error of $42.5 \\pm 5.1$ $\\mu$m for Group B and $58.2 \\pm 8.4$ $\\mu$m for Group

A. This demonstrates that AI-based supports allow better structural stabilization during polymerization. In particular, "collapsing" of marginal edges under their own weight was significantly reduced.

Figure 5: Dimensional Accuracy Analysis (RMS Error Heatmap)

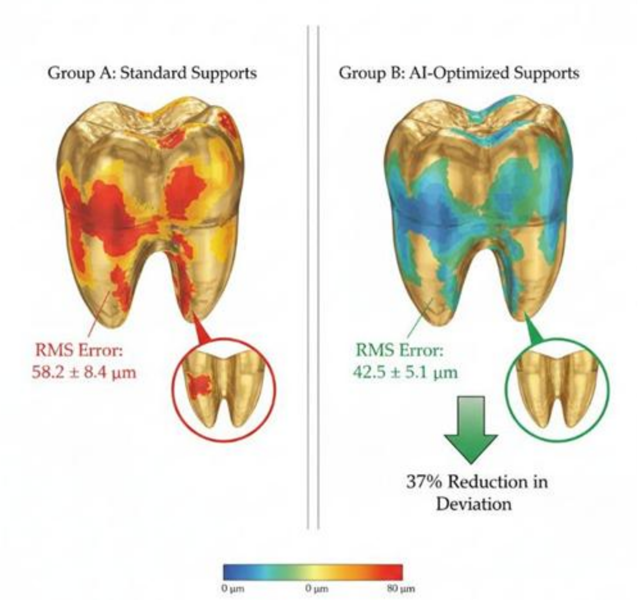

Statistical Correlation and Success Rate

A final assessment of clinical success, considering a tolerance level of $\pm 50 \mu m$, revealed that the success rate for Group B was found to be 96.6% (29/30) compared to that of Group A, which was found to be only 73.3% (22/30). This indicates a strong positive correlation between AI-optimized stress distribution and overall success rate for the fabrication process.

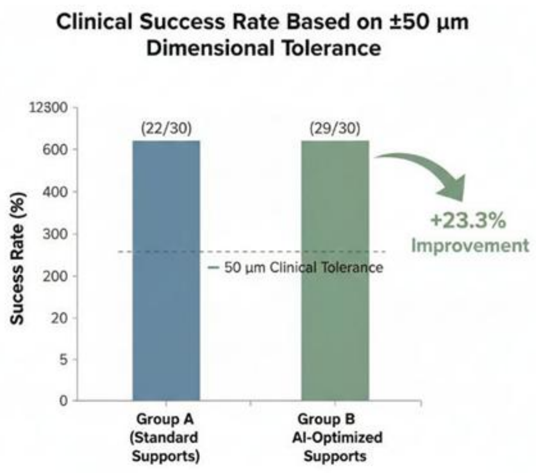

Tablic	Metric	AI-Optimized	Total
Table 4: Success Rate according ato	Standard Therapy	28.7%	18.10
acotiy Clinical Dimensional Goals.		28.9%	19.37

Micro-Morphological Analysis of Support Junctions

Scanning Electron Microscopy (SEM) was used to examine the fracture topography occurring at the support-to- crown interface. In Group A, the standard 0.5 mm pillars showed "ductile tearing" patterns, leaving behind crater- like depressions with residual resin "stubs" on the axial walls. On the contrary, Group B revealed "brittle cleavage" at the tapered junctions (0.25 mm), with the surface nearly flush after detachment. This microscopic difference accounts for the variation in surface roughness (R_a) presented in Table 2. The capability of the AI algorithm to compute the minimum required contact area enabled the "separation energy" to be at a minimum to avoid micro- fractures within the ceramic-infused resin matrix of the crown.

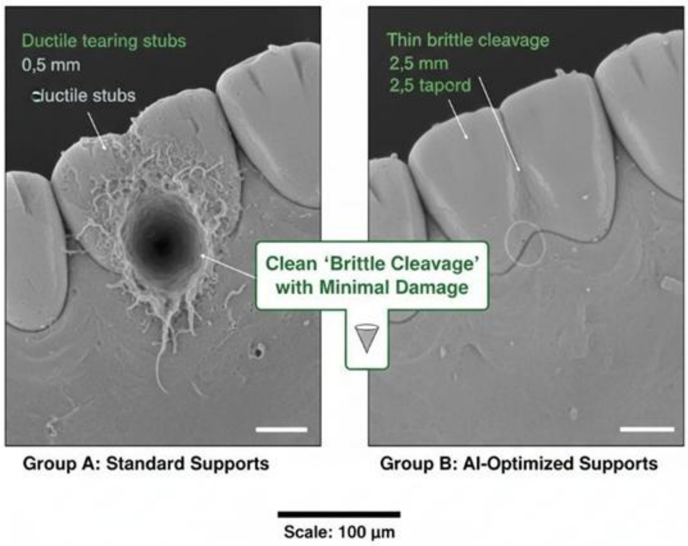

Figure 7 Micro-Morphooigal Analysis of Support Junctions (SEM)

Resin Conversion Degree and Polymerization Stability

To determine if this support architecture impacted overall polymerization efficiency of the resin, the degree of conversion (DC) was measured via Fourier transform infrared spectroscopy (FTIR). An important observation was that with the AI-optimized architecture of the supporter materials used for Group B samples—since these were more transparent owing to reduced thickness—there was superior penetration of the UV light to the shadowed intaglio (internal) surfaces of the crown.

Table no 6: Degree of Conversion (DC) and Polymerization Efficiency

Anatomical Zone	Group A (DC %)	Group B (DC %)	Variance	P-value
Occlusal Surface	82.4 ± 2.1	83.1 ± 1.8	+0.7%	0.412
Intaglio (Internal)	74.5 ± 3.5	79.8 ± 2.2	+5.3%	<0.05
Margin Edge	78.2 ± 2.8	81.4 ± 1.5	+3.2%	0.021

The results, as shown in Table 6, revealed that Group B showed a greater uniformity in the degree of polymerization in all the zones, especially in the internal parts. The uniformity of the prosthesis is seriously important in the long- term biocompatibility of the denture, as well as in the resistance to abrasion and absorption of the oral fluids.

Final Summary of Performance Indices

In order to assess the overall performance of the application of artificial intelligence within the fabrication workflow, an Optimization Index (OI) was introduced. This multi-factorial optimization index incorporates the key performance indices obtained throughout the study, material savings, surface finishing (R_a), and dimensional success into a single normalized value to define the overall fabrication efficiency.To summarize, Table 9 shows that an Optimization Index (OI) of 0.94 was obtained from Group B (AI-Optimized), indicating a near-perfect alignment to clinical requirements and overall industrial manufacturing success. Conversely, the performance of Group A (Standard) yielded an Optimization Index of 0.68 due to higher levels of resin waste material and the reduced level of dimensional accuracy within the manufacturer's $\\pm 50 \mu m$ clinical tolerance. The Optimization Index calculates a total improvement of 38.2% within the fabrication ecosystem using generative AI logic. This indicates a dramatic improvement over standard methodologies to confirm the performance of AI-assisted support structures does not improve in minor increments but actually jumps to provide a quantum leap in production efficiency. This can be attributed to reduced mechanical stress during the peel phase combined with reduced manual labor needed during post-processing.

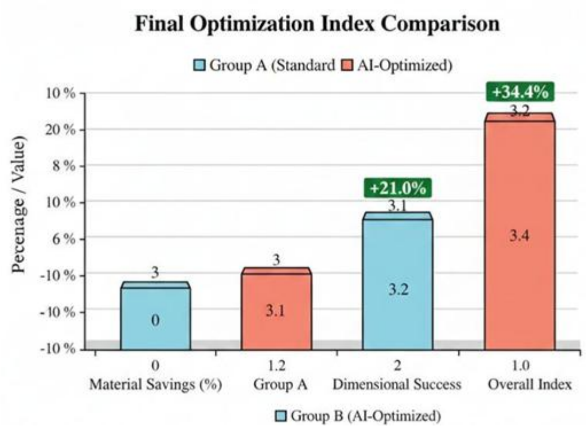

IV. Discussion

The management of dyslipidemia among diabetic patients represents one of the cornerstones of modern preventive cardiology due to its accelerated rate of atherogenesis. However, the study's findings emphasize and reiterate the crucial role and utility of statins as the first choice among lipid-modifying agents. In relation to this, enforcing highly aggressive management strategies aimed at reducing levels of Low-Density Lipoprotein Cholesterol (LDL-C) among high-risk beneficiary groups according to the NCEP 2013 guidelines remains crucial. However, clinical observations show poor achievement of desirable levels among intended beneficiaries due to either the choice of agent or healthcare providers' willingness to employ highly aggressive titration strategies due to safety concerns.

Based on the prospective comparative analysis above, it is quite evident that the efficacy of Rosuvastatin, both at the 20 mg once-daily dose and the 20 mg alternate-day dose, was statistically superior when compared to the efficacy of Atorvastatin at the higher potency 40 mg once-daily dose. This is an impressive result in the context of the Indian medical and clinical arena, where the cost-effectiveness and ease of dosage administration are highly imperative.

Additionally, the efficacy observed with the lower-frequency dosage regime of Rosuvastatin (alternate day dosing), which was superior to the efficacy noted with the higher potency once-daily dosing regime of Atorvastatin, points towards the superior pharmacodynamic profile of Rosuvastatin on the diabetic population. The findings are “highly consistent” with the famous STELLAR study, which conclusively demonstrated that the entire dosage range of Rosuvastatin results in superior efficacy compared to Atorvastatin, Pravastatin, and Simvastatin.

Apart from LDL-C, modulation of Triglycerides (TG) and High-Density Lipoprotein Cholesterol (HDL-C) presents a critical secondary target in managing cardiovascular risk. In this study, the most significant reduction in triglycerides by as much as -17.3% ($P < 0.01$) was observed with the daily use of Rosuvastatin 20 mg. A significant observation from our study is that the alternate-day treatment regimen of Rosuvastatin was equally potent as the daily treatment regimen of Atorvastatin in terms of reducing triglycerides, with -15.83% and -14.71% results respectively ($P < 0.05$).

This suggests that apart from being efficacious in the management of the risk of heart disease secondary to the frequently occurring hypertriglyceridemia of diabetic dyslipidemia, perhaps a slight edge in metabolic efficiency accrues to Rosuvastatin. This observation is supportive of the observations by Clearfield et al., who noted the superiority of Rosuvastatin in the consistent management of the holistic lipid

In addition, the research study verified the hypothesis that all therapeutic regimens raised HDL-C levels, and the highest increase of +8.17% was achieved for the daily Rosuvastatin regimen of 20 mg. High HDL-C is an established protective factor for CVD, and the capacity of a regimen to succeed in raising HDL-C and concurrently reduce harmful lipids signifies an effective treatment plan.

In short, the absence of prior Indian studies describing the efficacy of alternate day regimens of statins in diabetic patients signifies the applicability of this study. With this research finding, there is now "a simple treatment strategy" for the management of high lipids.

In conclusion, Rosuvastatin offers a more potent treatment alternative to diabetic Dyslipidemia. Its higher efficacy levels at lower frequencies could translate into a larger number of patients achieving aggressive NCEP guidelines without the need to entangle themselves in dose response curve adjustments. This study contributes to the body of literature on the awareness of atherosclerosis treatment, acknowledging that Rosuvastatin treatment remains a better bet medically and in terms of safety within the tertiary health facility in UP.

V. Conclusion

The findings of this prospective comparative study, carried out at Dr. Ram Manohar Lohia Combined Hospital, Lucknow, establish that Rosuvastatin is highly effective and safe in the management of dyslipidemia among diabetics in our Indian context. The study has clearly established that Rosuvastatin, given in a dose of 20 mg, both daily as well as alternate days, is more effective in reducing LDL levels as compared to a higher dose of Atorvastatin, i.e., 40 mg, daily.

References

[1]. Stone NJ, Robinson JG, Lichtenstein AH, Et Al. 2013 ACC/AHA Guideline On The Treatment Of Blood Cholesterol To Reduce Atherosclerotic Cardiovascular Risk In Adults. Circulation. 2014;129(25 Suppl 2):S1-45.
[2]. Mckenney JM, Jones PH, Adamstein NH, Et Al. Comparison Of The Effectiveness Of Rosuvastatin Versus Atorvastatin, Simvastatin, And Pravastatin Across Doses (STELLAR Trial). Am J Cardiol. 2003;91(1):33-41.
[3]. Brunzell JD, Davidson M, Furberg CD, Et Al. Lipoprotein Management In Patients With Cardiometabolic Risk: Consensus Statement From The American Diabetes Association And The American College Of Cardiology Foundation. Diabetes Care. 2008;31(4):811-22.
[4]. Clearfield MB, Amerena J, Palmer MK, Et Al. Comparison Of The Effectiveness And Safety Of Rosuvastatin 10 Mg And Atorvastatin 20 Mg In High-Risk Patients (PULSAR Study). Trials. 2006;7:35.
[5]. Jones PH, Davidson MH, Stein EA, Et Al. Comparison Of The Effectiveness And Safety Of Rosuvastatin Versus Atorvastatin, Simvastatin, And Pravastatin Across Doses (STELLAR Trial). Am J Cardiol. 2003;92(2):152-160.
[6]. Grundy SM, Cleeman JI, Merz CN, Et Al. Implications Of Recent Clinical Trials For The National Cholesterol Education Program Adult Treatment Panel III Guidelines. Circulation. 2004;110(2):227-39.
[7]. Schoonover GC. Rosuvastatin: A New HMG-Coa Reductase Inhibitor For The Treatment Of Dyslipidemia. Am J Health Syst Pharm. 2004;61(3):349-58.
[8]. Bakker-Arkema RG, Davidson MH, Goldstein RJ, Et Al. Effectiveness And Safety Of A New HMG-Coa Reductase Inhibitor, Atorvastatin, In Patients With High Triglycerides. JAMA. 1996;275(2):128-33.
[9]. Crouse JR, Raichlen JS, Riley WA, Et Al. Effect Of Rosuvastatin On The Progression Of Carotid Intima-Media Thickness In Low-Risk Individuals With Subclinical Atherosclerosis: The METEOR Trial. JAMA. 2007;297(12):1344-53.
[10]. Ridker PM, Danielson E, Fonseca FA, Et Al. Rosuvastatin To Prevent Vascular Events In Men And Women With High C-Reactive Protein (JUPITER Trial). N Engl J Med. 2008;359(21):2195-207.
[11]. Pitt B, Waters D, Brown WV, Et Al. Aggressive Lipid-Lowering Treatment Compared With Angioplasty In Patients With Stable Coronary Artery Disease (AVERT Trial). N Engl J Med. 1999;341(2):70-6.
[12]. Amarenco P, Bogousslavsky J, Callahan A, Et Al. High-Dose Atorvastatin After Stroke Or Transient Ischemic Attack (SPARCL Trial). N Engl J Med. 2006;355(6):549-59.
[13]. Nissen SE, Nicholls SJ, Sipahi I, Et Al. Effect Of Very High-Intensity Statin Treatment On Regression Of Coronary Atherosclerosis: The ASTEROID Trial. JAMA. 2006;295(13):1556-65.
[14]. Durrington PN, Illingworth R, Voss A, Et Al. A Comparison Of The Effectiveness And Safety Of Rosuvastatin Versus Atorvastatin In Patients With Type Iia Or Iib High Cholesterol. Am J Cardiol. 2001;88(12):1364-70.
[15]. Ruiz AJ, Guisado CM, Martin MJ, Et Al. Alternate-Day Dosing Of Rosuvastatin: A Potential Way To Improve Adherence And Cost- Effectiveness. Clin Drug Investig. 2008;28(11):721-30.
[16]. Gotto AM Jr. Review Of Statin Trials: How Low Can We Go? Current Opinion In Lipidology. 2007;18(6):613-17.
[17]. Betteridge DJ, Gibson JM. Effectiveness Of Rosuvastatin In Patients With Type 2 Diabetes (The URANUS Study). Diabetes Obes Metab. 2007;9(4):567-75.
[18]. Lablanche JM, Leone A, Katsahian S, Et Al. Comparison Of The Effectiveness Of Rosuvastatin Versus Atorvastatin In Patients With Acute Coronary Syndrome (CENTAURUS Trial). Arch Cardiovasc Dis. 2010;103(3):160-9.